Overexpression of Kinase-Dead mTOR Impairs Glucose Homeostasis by Regulating Insulin Secretion and Not β-Cell Mass

Emilyn U. Alejandro,[1,2] Nadejda Bozadjieva,[1] Manuel Blandino-Rosano,[1,3] Michelle Ann Wasan,[2] Lynda Elghazi,[1] Suryakiran Vadrevu,[4] Leslie Satin,[4] and Ernesto Bernal-Mizrachi[1,3,5,6]

Diabetes 2017;66:2150–2162 | https://doi.org/10.2337/db16-1349

Regulation of glucose homeostasis by insulin depends on β-cell growth and function. Nutrients and growth factor stimuli converge on the conserved protein kinase mechanistic target of rapamycin (mTOR), existing in two complexes, mTORC1 and mTORC2. To understand the functional relevance of mTOR enzymatic activity in β-cell development and glucose homeostasis, we generated mice overexpressing either one or two copies of a kinase-dead mTOR mutant (KD-mTOR) transgene exclusively in β-cells. We examined glucose homeostasis and β-cell function of these mice fed a control chow or high-fat diet. Mice with two copies of the transgene [RIPCre; KD-mTOR (Homozygous)] develop glucose intolerance due to a defect in β-cell function without alterations in β-cell mass with control chow. Islets from RIPCre;KD-mTOR (Homozygous) mice showed reduced mTORC1 and mTORC2 signaling along with transcripts and protein levels of Pdx-1. Islets with reduced mTORC2 signaling in their β-cells (RIPCre;Rictor$^{fl/fl}$) also showed reduced Pdx-1. When challenged with a high-fat diet, mice carrying one copy of KD-mTOR mutant transgene developed glucose intolerance and β-cell insulin secretion defect but showed no changes in β-cell mass. These findings suggest that the mTOR-mediated signaling pathway is not essential to β-cell growth but is involved in regulating β-cell function in normal and diabetogenic conditions.

Pancreatic β-cell failure, involving impaired insulin secretion and decreased β-cell mass, is a major hallmark of type 2 diabetes. The capacity of β-cells to adapt to increased insulin demand (i.e., to efficiently produce and secrete insulin) is a critical factor in the pathogenesis of this disease. The molecular mechanisms and signals driving how β-cells adapt to conditions of insulin resistance have not been completely elucidated. Given that insulin resistance is associated with states of overnutrition and obesity, we hypothesize that the nutrient environment and alterations in different nutrients in circulation modulate the adaptation of β-cells to obesity and insulin resistance. The mammalian target of rapamycin (mTOR) senses nutrients, energy, growth factors, and environmental cues to transmit signals to downstream targets to regulate multiple biological processes. However, how mTOR signaling inactivation impacts on β-cell mass and function in vivo has not been explored.

mTOR exists in two distinct complexes, mTORC1 and mTORC2, and regulates glucose homeostasis by modulating β-cell mass and function (1–4). mTOR complex 1, containing regulatory associated protein of mTOR (Raptor), is sensitive to rapamycin and regulates multiple biological processes by regulating S6K and eukaryotic translation initiation factor 4E binding protein. mTOR also forms complex 2 (mTORC2), which contains Rictor, thought to be insensitive to low-dose and short-term exposure to rapamycin, and is the kinase responsible for phosphorylating Akt on S473 (5). A significant amount of information about mTORC1 has been gained by the use of the immunosuppressant rapamycin. Studies using rapamycin have shown

[1]Division of Metabolism, Endocrinology & Diabetes, Department of Internal Medicine, University of Michigan, Ann Arbor, MI
[2]Department of Integrative Biology and Physiology, University of Minnesota, Minneapolis, MN
[3]Division of Endocrinology, Metabolism and Diabetes, University of Miami, Miami, FL
[4]Department of Pharmacology, University of Michigan, Ann Arbor, MI
[5]VA Ann Arbor Healthcare System, Ann Arbor, MI
[6]Miami VA Healthcare System, Miami, FL

Corresponding author: Ernesto Bernal-Mizrachi, ebernalm@med.miami.edu.

Received 3 November 2016 and accepted 1 May 2017.

This article contains Supplementary Data online at http://diabetes.diabetesjournals.org/lookup/suppl/doi:10.2337/db16-1349/-/DC1.

that this pathway regulates β-cell growth, proliferation, size, protein translation, and insulin secretion (6,7). However, there are many limitations to the use of this inhibitor including specificity and differential inhibition of downstream targets (8). In addition, gain-of-function mTORC1 through β-cell deletion of tuberous sclerosis complex 1 or 2 has a positive impact on proliferation and β-cell mass (1,2). Overexpression of the protein Ras homolog enriched in brain (Rheb), a Ras-like small GTPase that activates mTORC1, also promotes β-cell growth (by increasing cell size) and higher insulin secretion (9). Loss of the other mTOR complex, mTORC2, by conditional Rictor deletion in β-cells leads to insulin secretion dysfunction (4). Although these genetic models have been valuable in understanding the function of different mTOR complexes, the effect of conditional inactivation of mTOR (both mTORC1 and mTORC2) in pancreatic β-cells is unknown. In addition, a major limitation for studying mTOR in physiology has been the lethality of global mTOR-deficient mice. Therefore, developing β-cell models of partial decrease in function that could reflect more physiological conditions can provide critical information about the role of this nutrient sensor in β-cells.

The goal of the current study was to determine the effects of incomplete loss of β-cell mTOR (both complex 1 and complex 2) activity on glucose homeostasis and β-cell mass and function with basal and high-fat diet (HFD) conditions. Using Tet-off inducible mice overexpressing a kinase-dead mTOR mutant in β-cells (RIPCre;KD-mTOR), we identified a role of mTOR in glucose homeostasis due to a defect in β-cell function, and unexpectedly, without alterations in β-cell mass. We found that RIPCre; KD-mTOR mice exhibited defective adaptation to HFD mainly by alterations in insulin secretion. Interestingly, we showed that the defects in insulin secretion by inhibition of mTOR signaling were caused in part by the decrease in Pdx-1 levels, identifying a novel mTOR–Pdx-1 axis in β-cells.

RESEARCH DESIGN AND METHODS

Animal Generation

Constitutive overexpression of RIPCre;KD-mTOR was achieved by breeding mice harboring the transgene (KD-mTOR) (Fig. 1*A*) with RIP-Cre^{Herr} mice (10). The pcDNA3/mTOR eukaryotic expression plasmid encoding kinase-dead (D2338A) mTOR was generated as described previously (11). The kdmTOR transgene construct used to generate these mice was built on a backbone knock-in single cassette vector for the ROSA26 locus and contains the splice-acceptor sequence, neomycin cassette, tetracycline transactivator (tTA) gene, insulator sequence, CMV promoter responsive to tTA, rabbit β-globin intron, kdmTOR cDNA, internal ribosome entry site, and enhanced green fluorescence protein (EGFP) cDNA (Fig. 1*A*). The linearized vector was electroporated into embryonic stem cells by the University of Michigan Transgenic Animal Model Core. After neomycin selection, three clones were karyotyped and used for blastocyst injection to generate chimeric mice (12). After identifying germline transmission, two independently derived founder lines were selected and bred into C57BL/6J background. Both lines had similar phenotypes and one line was used to generate all the experiments presented here. Mice were bred to contain one copy (heterozygous [Het] allele) or two copies (homozygous [Homo] alleles) of the transgene. In this Tet-off model, expression of the tTA is turned on upon Cre-mediated recombination, and removal of the neo gene cassette induces KD-mTOR expression in the absence of doxycycline. Genotyping of all mice was performed by PCR using DNA from tail biopsy (primer sequences available upon request). Raptor$^{fl/fl}$ and Rictor$^{fl/fl}$ mice were a generous gift from Drs. Michael N. Hall and Marcus A. Rüegg at the University of Basel, Basel, Switzerland (13,14). The University of Michigan and University of Miami Animal Studies Committees approved all the procedures.

Islet Isolation, cAMP, and Insulin Secretion Assay

Primary mouse islets from RIPCre;KD-mTOR (Homo) mice were isolated using collagenase (1 mg/mL, Roche Applied Science) and handpicked after filtration with a 70-μm cell strainer (BD Falcon) as described previously (15). The islets were allowed to recover in RPMI media supplemented with 5 mmol/L glucose and 10% FBS overnight.

Insulin secretion ex vivo was assessed using isolated islets by static incubation. Briefly, after overnight culture in RPMI containing 5 mmol/L glucose, groups of 10 islets/mouse were placed in 8-μm cell culture inserts (Millicell), preincubated in low-glucose KREB (2 mmol/L glucose) for 1 h, and incubated subsequently for 30 min in each experimental condition. Secreted insulin levels and islet insulin content were measured with an ELISA (ALPCO Mouse Ultrasensitive Insulin ELISA). All data are represented as secreted insulin in the culture medium normalized to islet insulin content for each insert of islets and presented as fold change. cAMP levels were measured in islets from mice overexpressing the mutant KD-mTOR and control. Isolated islets were allowed to recover overnight in RPMI media supplemented with 10% FBS and 5 mmol/L glucose. The next day islets were incubated for 1 h in RPMI without serum and 2 mmol/L glucose at 37°C as recommended by the cAMP-Glo Assay Kit (Promega). Twenty islets (n = 6 per group) were placed in a 96-well plate and exposed to either 2 or 16 mmol/L glucose for 15 min. Islets were then lysed using lysis buffer provided in the kit and cAMP levels were measured using the Promega GloMax Discover luminometer per kit instructions.

Western Blotting

Immunoblotting was performed as described previously (15). Briefly, islet cells were washed after treatments with PBS before adding cell lysis buffer (Cell Signaling) with protease inhibitor cocktail and PhosStop tablets (Roche Applied Science). Primary antibodies against GFP, phosphorylated S6 (Ser240) and Akt (Ser473), and total Akt were purchased

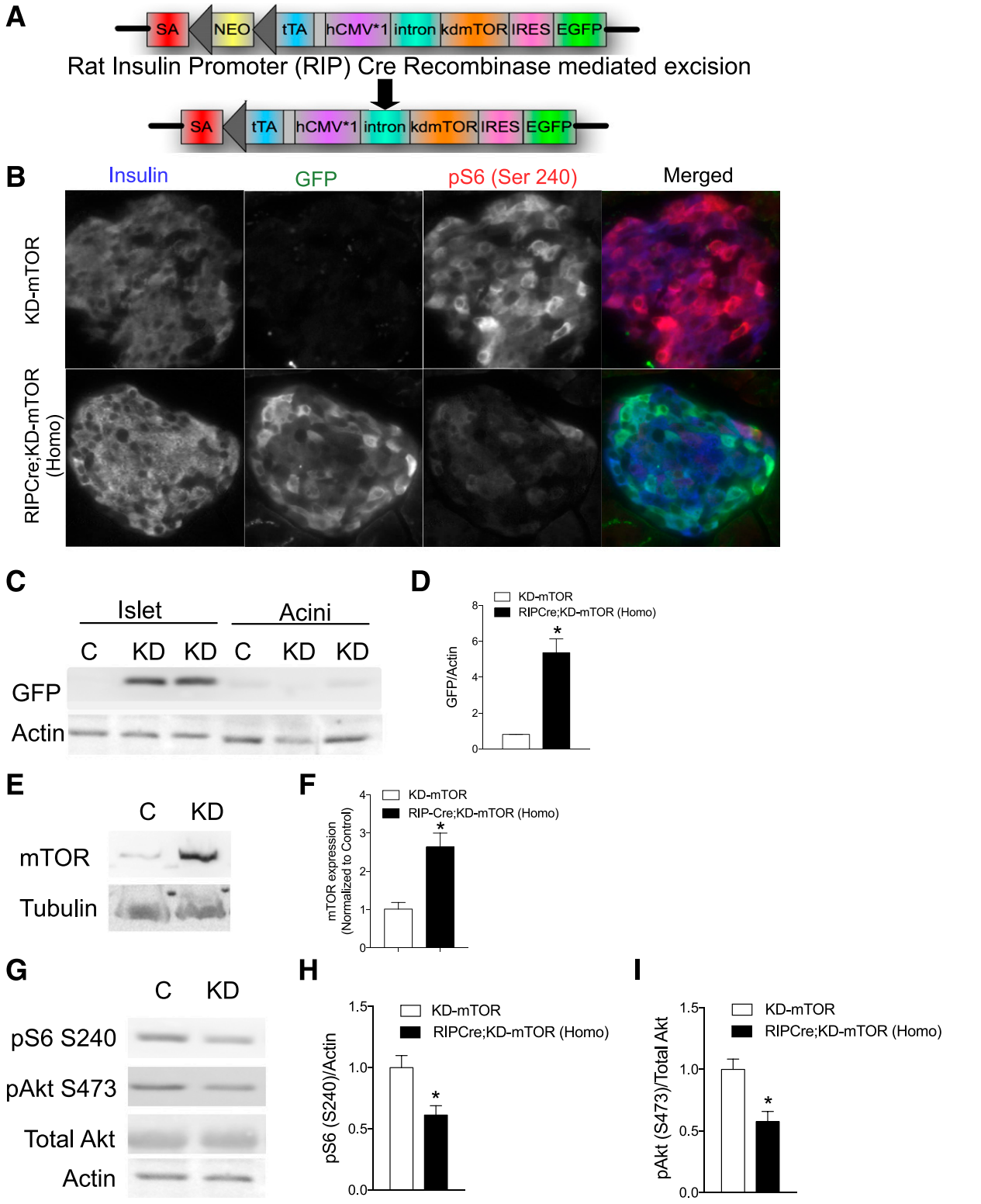

Figure 1—Expression of KD-mTOR mutant in β-cells reduces S6 phosphorylation. *A*: Transgene construct of the KD-mTOR and generation of β-cell–specific RIPCre;KD-mTOR mice. IRES, internal ribosome entry site; NEO, neomycin cassette; SA, splice-acceptor sequence. *B*: Recombination efficiency was assessed by EGFP expression in islets of RIPCre;KD-mTOR (Homo) mice. Adult pancreas was stained for insulin (blue), phosphorylated S6 (S240) (red), and GFP (green). Images shown are 40× magnification. *C* and *D*: Increased expression of GFP (transgene reporter) by Western blotting (*C*) in islets and acini from 3-month-old male RIPCre;KD-mTOR (Homo) (KD) and control (C) mice. Quantification of GFP to Actin is shown in *D*, $n = 3$. *E* and *F*: Immunoblotting and quantification for mTOR levels in adult islets from RIPCre;KD-mTOR (Homo) and control mice. *G–I*: Reduced phosphorylated S6 (S240) (*G* and *H*) and phosphorylated Akt (S473) (*G* and *I*) in adult islets from RIPCre;KD-mTOR (Homo) compared with control mice. Quantification is shown for phosphorylated S6 (S240) (*H*) and phosphorylated Akt (S473) (*I*). *$P < 0.05$ between RIPCre;KD-mTOR and control mice unless otherwise indicated. Statistical analyses were conducted using unpaired, nonparametric Mann-Whitney *U* test.

from Cell Signaling. Pdx-1 antibody was purchased from Millipore. Antibodies against β-actin and tubulin were purchased from Sigma.

Pancreatic β-Cell Mass and Proliferation Analysis

Formalin-fixed pancreas tissues were embedded in paraffin. Sections were deparaffinized, rehydrated, and incubated with blocking solution as previously described (15). Sections were incubated overnight at 4°C with antibodies against insulin (Dako) and Ki67 (Millipore), followed by secondary antibodies conjugated to FITC and Cy3 (Jackson ImmunoResearch). DAPI-containing mounting media (Vector Laboratories) was added to coverslips. β-Cell mass analysis entailed assessing total pancreas and insulin-positive cell areas from five insulin-stained sections (5 μm) separated by 200 μm and measured by using Image-Pro software (Media Cybernetics). β-Cell mass (average β-cell fraction multiplied by pancreas weight) assessment was performed using Surveyor software (Objective Imaging) automated scanning with a Leica fluorescent microscope (Leica Microsystems). Cell proliferation was analyzed using costaining of Ki67 with insulin on tissue sections of control and transgenic mice. Apoptotic cells in insulin-positive cells were assessed using the ApopTag Red In Situ Apoptosis Detection kit (Millipore) on tissue sections of control and transgenic mice.

Glucose and Insulin Tolerance Tests

Fasting glucose levels were measured after 12-h overnight fasting. Glucose tolerance was assessed by intraperitoneal (IP) delivery of 2 g/kg glucose to mice after 12-h fasting. Insulin tolerance test was assessed by IP delivery of 0.75 unit/kg insulin (Humalog; Eli Lilly) to mice after 6-h fasting. Blood glucose was monitored every 30 min for 2 h after glucose or insulin injection using the AlphaTRAK glucose meter. Plasma insulin levels were collected and measured using Ultrasensitive Mouse Insulin ELISA Kit (ALPCO).

Measurement of Intracellular Ca^{2+}

Isolated islets were allowed to recover overnight from islet isolation prior to measurement of intracellular Ca^{2+}. Islets were preloaded with 2.5 μmol/L Fura2-AM (molecular probes) in 0.1% DMSO for 30 min at 37°C and washed for 10 min before recording. The recording solution contained, in mmol/L, 145 NaCl, 5 KCl, 1.2 $MgCl_2$, 2.6 $CaCl_2$, 10 HEPES, and glucose as indicated. pH 7.4. Ca^{2+} is reported as the ratio of alternative excitation at 340 nm/380 nm, with emission measured at 510 nm.

Statistical Analysis

All values are expressed as mean ± SEM. Statistical analyses were conducted using unpaired, nonparametric Mann-Whitney *U* test or ANOVA followed by post hoc analysis, where appropriate, by using GraphPad Prism (version 6.0c, GraphPad Software, La Jolla, CA). Results were considered significant with a $P \leq 0.05$.

RESULTS

Expression of KD-mTOR Mutant in β-Cells Reduces S6 Phosphorylation

To determine the impact of reduced mTOR signaling on β-cells, we generated a mouse with constitutive overexpression of KD-mTOR mutant. After Cre recombination, tTA transcription is activated and induces expression of a KD-mTOR mutant (Asp2338 to Ala mutation) and EGFP, allowing visualization of KD-mTOR–expressing cells. To induce KD-mTOR expression specifically in β-cells, we crossed the KD-mTOR and RIP (rat insulin promoter) Cre transgenic mice (9) (Fig. 1*A*). To assess the effect of dose response inhibition of mTOR, we generated two KD-mTOR transgenic lines: one with one copy of the transgene, RIPCre;KD-mTOR (Het), and one with two copies, RIPCre; KD-mTOR (Homo). Functionality of the system in vivo was demonstrated by immunofluorescence for EGFP and insulin in RIPCre;KD-mTOR (Homo) and control mice (Supplementary Fig. 1*A*). EGFP fluorescence was demonstrated exclusively in β-cells (Supplementary Fig. 1*A*) but not in α-cells from RIPCre;KD-mTOR mice at postnatal day 0 (Supplementary Fig. 1*B*). We found that approximately 80% of insulin-producing cells express GFP in neonate RIPCre; KD-mTOR (Homo) mice (Supplementary Fig. 1*C*). Then, we analyzed EGFP expression to assess the levels of the mutant KD-mTOR expression in adult mice. β-Cells from RIPCre;KD-mTOR (Het) mice exhibited positivity for EGFP in β-cells (Supplementary Fig. 2*A*). RIPCre;KD-mTOR (Homo) mice exhibited a more robust expression of EGFP (Fig. 1*B* and Supplementary Fig. 2*B*) compared with RIPCre; KD-mTOR (Het) mice (Supplementary Fig. 2*A*). Western blotting analysis showed EGFP expression only in islets from RIPCre;KD-mTOR (Homo) mice (Fig. 1*C* and *D*). No EGFP protein was detected in acinar cells from both control or RIPCre;KD-mTOR (Homo) mice (Fig. 1*C*). Islets from adult RIPCre;KD-mTOR (Homo) mice demonstrated a reduction in phosphorylated S6 (S240) staining in EGFP and insulin-positive cells (Fig. 1*B*) and phosphorylation levels by Western blotting (Fig. 1*E* and *F*). Phosphorylation of mTORC1 and mTORC2 targets, S6 (S240) protein and Akt (S473), respectively, were reduced in islets from adult RIPCre; KD-mTOR (Homo) mice indicating that expression of the KD-mTOR mutant transgene reduced mTOR signaling (Fig. 1*G–I*). These data demonstrated successful generation of a mouse model with dox-regulated expression of a KD-mTOR mutant and inhibition of mTORC1 and mTORC2 signaling.

RIPCre;KD-mTOR (Homo) Mice Exhibit Normal Islet Architecture and β-Cell Mass in Neonates

Neonatal RIPCre;KD-mTOR (Homo) mice were viable and indistinguishable from wild-type control mice, without alteration in body weight and length and circulating glucose levels (Fig. 2*A–C*). In addition, the β-cell area between RIPCre;KD-mTOR (Homo) and control neonates was comparable (Fig. 2*D*). Because this was an unexpected result, we next assessed the β-cell area in neonates lacking either mTORC1 or mTORC2 by deleting Raptor or Rictor, respectively, in

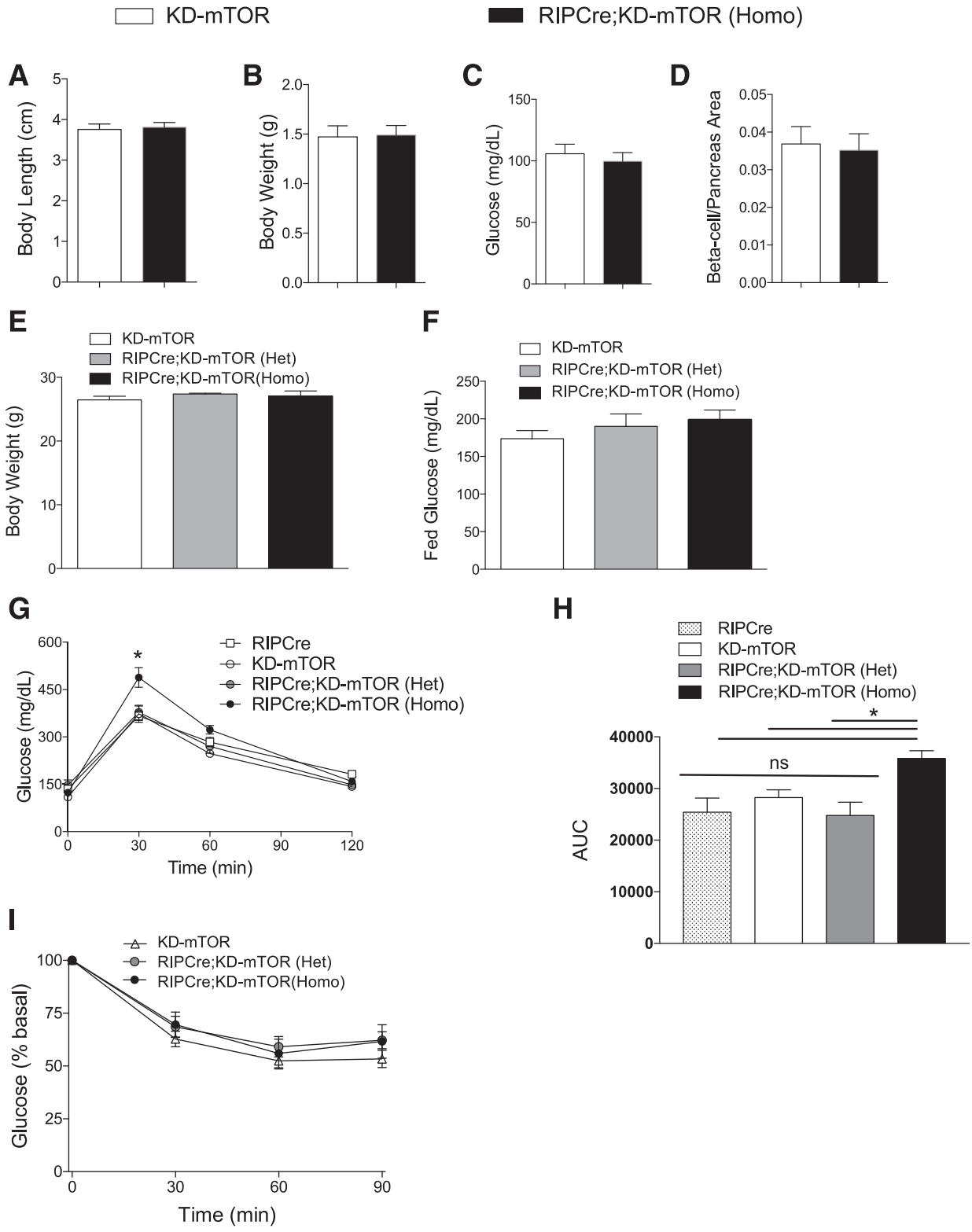

Figure 2— RIPCre;KD-mTOR mice exhibit normal islet architecture and β-cell mass in neonates and glucose intolerance later in life. *A–C*: Body length, body weight, and glucose levels in newborn RIPCre;KD-mTOR (Homo) and control mice. *D*: β-Cell area (insulin positive)/pancreas area ratio between RIPCre;KD-mTOR (Homo) and littermate control mice. *E* and *F*: Normal body weight (*E*) and random blood glucose (*F*) levels in RIPCre;KD-mTOR (Het), RIPCre;KD-mTOR (Homo), and control mice. *G*: Twelve-week-old male RIPCre;KD-mTOR (Homo) mice showed impaired glucose tolerance via IP compared with RIPCre;KD-mTOR (Het) and littermate control mice fed a normal chow diet. *H*: Area under the curve (AUC) for G. *I*: Normal insulin sensitivity between all genotypes fed a normal chow diet. $n = 4–10$. Statistical analyses were conducted using two-way ANOVA in *E*, *F*, *G*, and *I*, showing only significant interaction and genotype differences between control and RIPCre;KD-mTOR (Homo) in *G*. Mann-Whitney *U* tests were done in *A–D* and *H* by prism. $^*P < 0.05$ between RIPCre;KD-mTOR and control mice, unless otherwise indicated.

β-cells. In accordance with the neonatal data in RIPCre;KD-mTOR (Homo) mice, there was no alteration in body weight, circulating glucose levels, and β-cell area between RIPCre;Raptor$^{fl/fl}$, RIPCre;Rictor$^{fl/fl}$, and control mice (Supplementary Fig. 3*A–F*). These data suggest that reduction of β-cell mTOR signaling during development is dispensable for β-cell development.

RIPCre;KD-mTOR (Homo) Mice Exhibit Glucose Intolerance

To determine the impact of mTOR inhibition in β-cells on glucose homeostasis in vivo, we assessed body weight and random glucose and performed glucose and insulin tolerance tests in 3-month-old male RIPCre;KD-mTOR (Het), RIPCre;KD-mTOR (Homo), and control mice. No significant changes in body weight were observed in RIPCre;KD-mTOR (Het) or RIPCre;KD-mTOR (Homo) mice compared with control mice indicating that potential leaky expression of the kdmTOR transgene in the hypothalamus was not physiologically significant to alter energy homeostasis (Fig. 2*E*). Fed glucose in RIPCre;KD-mTOR (Het) or RIPCre;KD-mTOR (Homo) mice was comparable to that of control mice (Fig. 2*F*). However, RIPCre;KD-mTOR (Homo) transgenic mice exhibited glucose intolerance when compared with RIPCre;KD-mTOR (Het) and control mice (Fig. 2*G* and *H*). No differences in insulin sensitivity between genotypes were observed (Fig. 2*I*). Together, these data suggest that RIPCre;KD-mTOR (Homo) mice exhibit normal islet architecture and β-cell mass in neonates but develop glucose intolerance later in life.

RIPCre;KD-mTOR (Homo) Mice Have Normal β-Cell Mass and Insulin Content

Next, we assessed the contribution of β-cell mass to the alterations in glucose homeostasis observed in 3-month-old male RIPCre;KD-mTOR (Homo) mice. β-Cell mass and architecture between adult RIPCre;KD-mTOR (Homo) and control mice was comparable (Fig. 1*C*, Supplementary Fig. 2*B*, and Fig. 3*A*). No changes in the percentage of TUNEL-positive β-cells were observed between control and RIPCre;KD-mTOR mice (Fig. 3A'). We next determined if alteration of *insulin* and other important β-cell genes could contribute to the defect in insulin secretion. We observed a significant reduction of *insulin 1* and *insulin 2,* as well as *Pdx-1* transcription in islets from RIPCre;KD-mTOR (Homo) mice compared with control mice (Fig. 3*B–D*). No significant changes were observed in *MafA* and *NeuroD1* expression between the transgenic and control mice (Fig. 3*E* and *F*). Despite significant changes in *insulin* and *Pdx-1* mRNA, no alteration in insulin content was observed between RIPCre;KD-mTOR (Homo) and control mice (Fig. 3*G*). Together, these data suggest that reduced mTOR signaling caused by the KD-mTOR transgene is not sufficient to affect β-cell mass and insulin content.

RIPCre;KD-mTOR (Homo) Mice Show Impaired Insulin Secretion as a Result of Defects Distal to Calcium Influx

To further assess the mechanisms of alteration in glucose tolerance, we performed in vivo glucose-stimulated insulin secretion (GSIS) in 3-month-old male mice. RIPCre;KD-mTOR (Homo) mice showed abnormal insulin secretory responses after glucose load (Fig. 4*A*). Assessment of GSIS in vitro demonstrated impaired insulin secretory responses to high glucose in RIPCre;KD-mTOR (Homo) mice (Fig. 4*B*). Intracellular calcium concentration in response to high glucose was elevated in control mice, and these levels were not different than those of RIPCre;KD-mTOR (Homo) mice (Fig. 4*C* and *D*). Because insulin secretion can be augmented by cAMP-mediated metabolic or neurohormonal amplification, we assessed cAMP levels in response to glucose. Levels of cAMP (nmol/L per μg protein) in low glucose (2.754 ± 0.9743 vs. 2.599 ± 0.6674, $n = 6$, $P = 0.8$) or high glucose (fold change 7.253 ± 2.891 vs. 6.336 ± 4.056, $n = 6$, $P = 0.7$) were similar between control and islets overexpressing KD-mTOR, indicating that this pathway was not involved. These studies suggest that inhibition of mTOR signaling regulates distal events of insulin secretion.

Islets From RIPCre;KD-mTOR (Homo) Mice Have Reduced mTORC1 and mTORC2 Signaling, Which Was Associated With Decrease in Pdx-1 Protein Levels

To understand the mechanisms impinging on insulin secretion, we assessed the levels of mTORC1 and mTORC2 signaling. We assessed phosphorylated levels of S6 on S240 (an mTORC1-specific downstream target) and Akt on S473, a surrogate of mTORC2 activity (Fig. 1*E–G*). Islets from RIPCre;KD-mTOR (Homo) mice showed reduced phosphorylated S6 (S240) compared with control mice (Fig. 1*E* and *F*). Phosphorylated Akt (S473) was also reduced in RIPCre;KD-mTOR (Homo) mice without changes in total Akt levels (Fig. 1*E* and *G*). These data suggest that both mTORC1 and mTORC2 could be playing a role on the insulin secretory defect observed in the RIPCre;KD-mTOR mice. Pdx-1 is a critical transcription factor regulating pancreas development and β-cell function and survival, and recent data have shown that levels of this transcription factor are regulated by Akt/GSK3 signaling (16–21). We observed a significant reduction of Pdx-1 protein levels in islets from RIPCre;KD-mTOR mice (Fig. 5*A* and *B*). To further assess if the reduction of mTOR activity regulates Pdx-1 in an mTORC1 or mTORC2 manner, we evaluated the level of Pdx-1 in islets from mice with loss of mTORC1 (RIPCre;Raptor$^{fl/fl}$) or mTORC2 (RIPCre;Rictor$^{fl/fl}$) signaling specifically in β-cells. Pdx-1 protein was significantly reduced in nondiabetic RIPCre;Rictor$^{fl/fl}$ mice compared with control mice (Fig. 5*C* and *D*). In contrast, no alteration in Pdx-1 was observed in nondiabetic RIPCre;Raptor$^{fl/fl}$ islets (Fig. 5*C* and *E*). These data suggest that Pdx-1 protein reduction is downstream of mTORC2.

Abnormal Adaptation of RIPCre;KD-mTOR (Het) and RIPCre;KD-mTOR (Homo) Mice to HFD

To determine whether the decrease in mTOR signaling is important for β-cell adaptive responses to insulin resistance, we exposed these mice to HFD. No significant changes in fed or fasting glucose levels or body weight

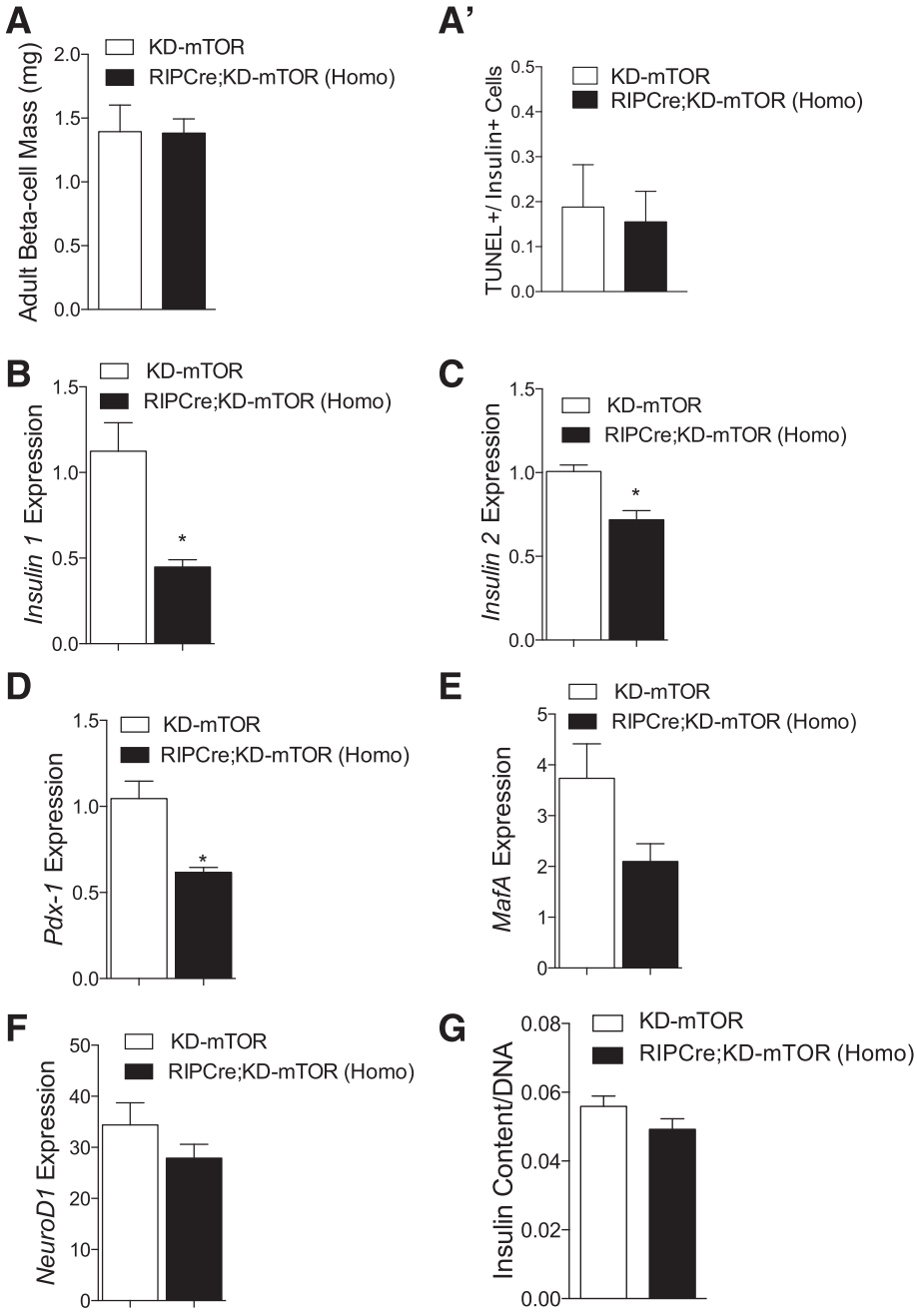

Figure 3—RIPCre;KD-mTOR mice have normal islet architecture, β-cell mass, and insulin content. *A*: Comparable β-cell mass between male RIPCre;KD-mTOR (Homo) and control mice. *A'*: RIPCre;KD-mTOR (Homo) and control islets showed normal levels of TUNEL$^+$/insulin$^+$ (apoptotic) cells. *B–D*: Significant reduction of *insulin 1*, *insulin 2*, and *Pdx-1* mRNA transcripts. *E* and *F*: No significant changes were detected in *MafA* and *NeuroD1* transcripts. *G*: Despite alterations in *insulin* and *Pdx-1* mRNA levels, insulin content in islets of RIPCre;KD-mTOR (Homo) mice showed no significant difference compared with littermate control mice. Statistical analyses were conducted using unpaired, nonparametric Mann-Whitney *U* test. *$P < 0.05$ between RIPCre;KD-mTOR (Homo) and control mice, $n = 4$.

were detected between male control and transgenic mice overexpressing one or two copies of the transgene (Fig. 6*A–C*). Fasting insulin levels between control mice and RIPCre;KD-mTOR (Homo) and RIPCre;KD-mTOR (Het) mice were comparable (Supplementary Fig. 4*A*). RIPCre; KD-mTOR (Homo) and RIPCre;KD-mTOR (Het) mice exhibited glucose intolerance after 4 and 16 weeks of HFD (Fig. 6*D* and *E*). An insulin tolerance test was performed after 10 weeks of HFD (Fig. 6*F*). In vivo insulin secretory response to glucose was markedly perturbed in RIPCre;KD-mTOR (Homo) and RIPCre;KD-mTOR (Het) mice after 16 weeks of HFD (Fig. 6*G*). β-Cell mass expansion after 16 weeks of HFD was similar among the groups suggesting that the degree of inhibition of mTOR signaling in these mice was not sufficient to alter the capacity of β-cells to expand mass in response to insulin resistance

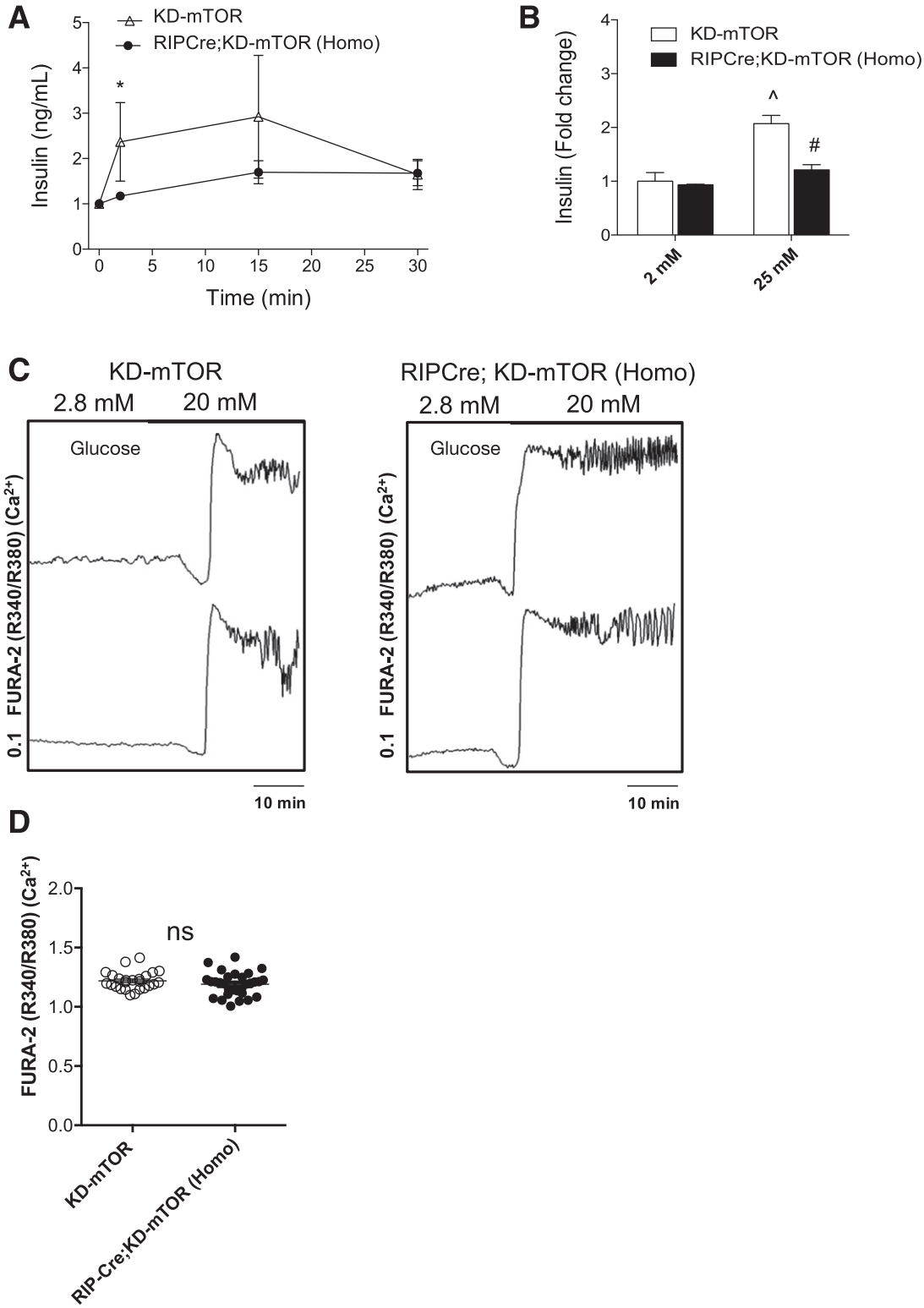

Figure 4—RIPCre;KD-mTOR mice show impaired insulin secretion as a result of defects distal to calcium influx. *A*: RIPCre;KD-mTOR (Homo) mice showed blunted insulin secretion compared with littermate control mice in response to high glucose in vivo. *B*: Islets from RIPCre;KD-mTOR (Homo) mice also demonstrated blunted insulin secretion in response to high glucose compared with littermate control mice in vitro. *C*: Example of intracellular Ca^{2+} traces in islets preloaded with Fura2-AM from 12-week-old RIPCre;KD-mTOR (Homo) mice in response to 20 mmol/L glucose. *D*: Quantification of Ca^{2+} traces, reported as the emission ratio R340/R380, in response to 20 mmol/L glucose, $n = 20$ islets. Statistical analyses were conducted using unpaired, nonparametric Mann-Whitney *U* test. *$P < 0.05$ between RIPCre;KD-mTOR (Homo) and control mice. ^$P < 0.05$ between low and high glucose response. #$P < 0.05$ between RIPCre;KD-mTOR and control mice in high-glucose conditions. $n = 5$ for in vivo GSIS and $n = 3$ for animals in both in vitro GSIS and Ca^{2+} studies (~18 islets per n were used).

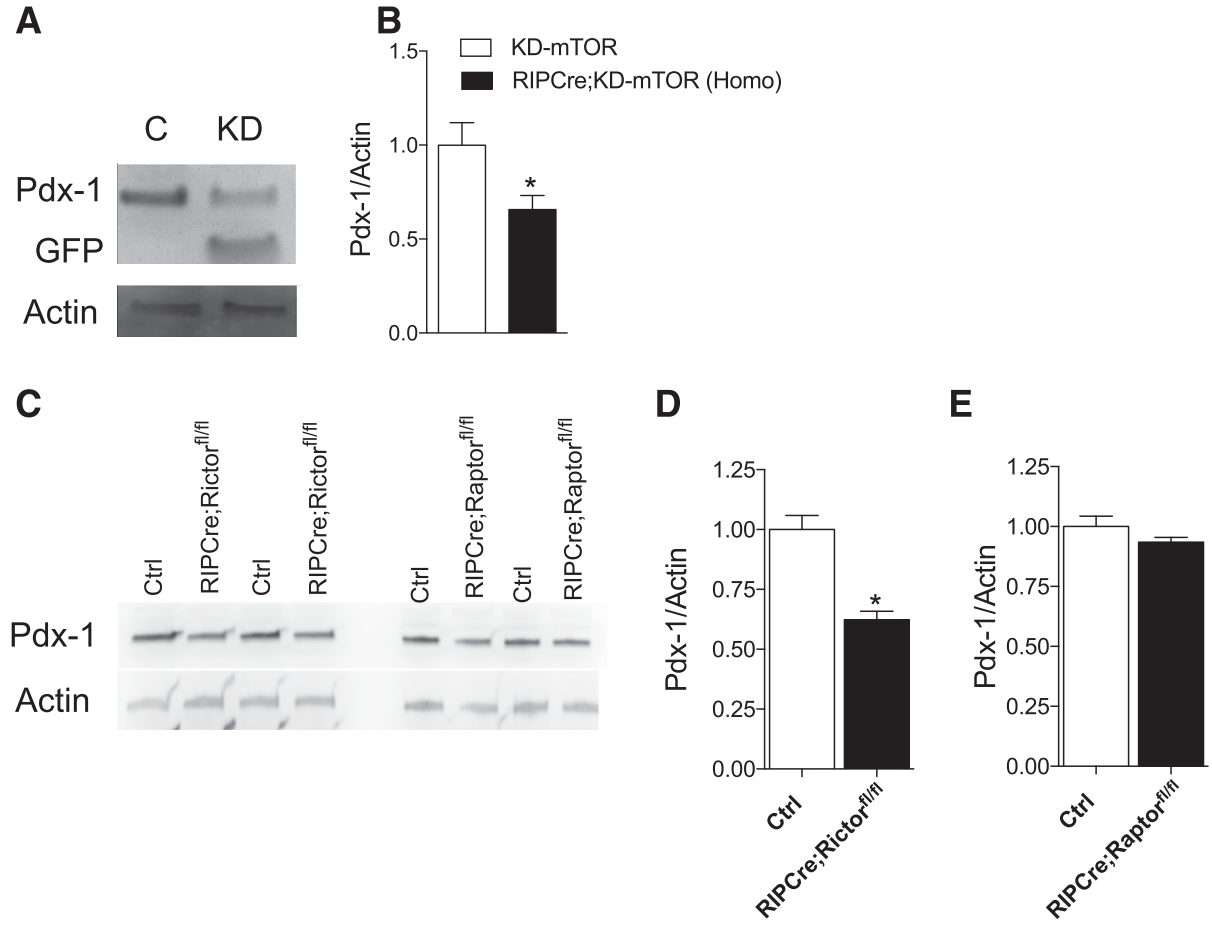

Figure 5—Islets from RIPCre;KD-mTOR mice have reduced Pdx-1 protein levels. *A* and *B*: Pdx-1 protein levels in islets from 4-month-old RIPCre;KD-mTOR (KD) compared with control (C) mice; quantification in *B*. *C*: Representative Western blots of Pdx-1 in islets from 3-month-old RIPCre;Rictor$^{fl/fl}$ and 1-month-old RIPCre;Raptor$^{fl/fl}$ mice compared with control (Ctrl) mice; quantification in *D* and *E*, respectively. Statistical analyses were conducted using unpaired, nonparametric Mann-Whitney *U* test. *$P < 0.05$, $n = 3$–6.

and overnutrition (Fig. 6*H*). We observed no differences in β-cell proliferation rate between genotypes (Supplementary Fig. 3*B*). Together, these data suggest that one copy of the KD-mTOR transgene is sufficient to induce glucose intolerance and insulin secretion defect in response to HFD. These findings also suggest that the mTOR-mediated signaling pathway is not essential to β-cell growth adaptation in response to HFD but is involved in regulating β-cell function.

DISCUSSION

mTOR kinase is involved in many cell processes including metabolism and cell growth. The use of the mTOR inhibitor, rapamycin, has shed light onto the role of mTOR in β-cells. However, the specificity of rapamycin and the partial effects on downstream targets are major limitations of this agent. Although published data evaluated the role of inactivation of mTORC2 in β-cells in vivo (4), the effect of concomitant decrease of mTORC1 and mTORC2 activity in β-cells has not been directly tested. The current study extends our current knowledge by assessing the effects of β-cell inactivation of mTOR function in glucose homeostasis and β-cell mass and function during basal conditions and after exposure to HFD. To understand the functional relevance of physiological loss of mTOR enzymatic activity in β-cell development and in glucose homeostasis in vivo, we generated a Tet-off mouse model overexpressing a KD-mTOR mutant in β-cells. This strategy allowed us to study a more physiological reduction of mTOR signaling and provided a unique assessment of the role of kinase activity of mTOR in regulating β-cell mass and function in vivo. These studies are the first in evaluating the effect of reduction of mTOR signaling in β-cells using genetic models and circumvent the limitations of in vivo and in vitro studies evaluating the effects of rapamycin in β-cells and glucose homeostasis.

Using RIPCre;KD-mTOR mice, we identified a role of mTOR on β-cell function. Given the known expression of Cre recombinase in brain and hypothalamus in this RIPCre line and the role of hypothalamic mTOR on appetite control, we examined weight in transgenic and control mice (22). We have not assessed mTOR expression in the hypothalamus, but no changes in weight were observed in RIPCre;KD-mTOR mice (Homo or Het) fed control chow

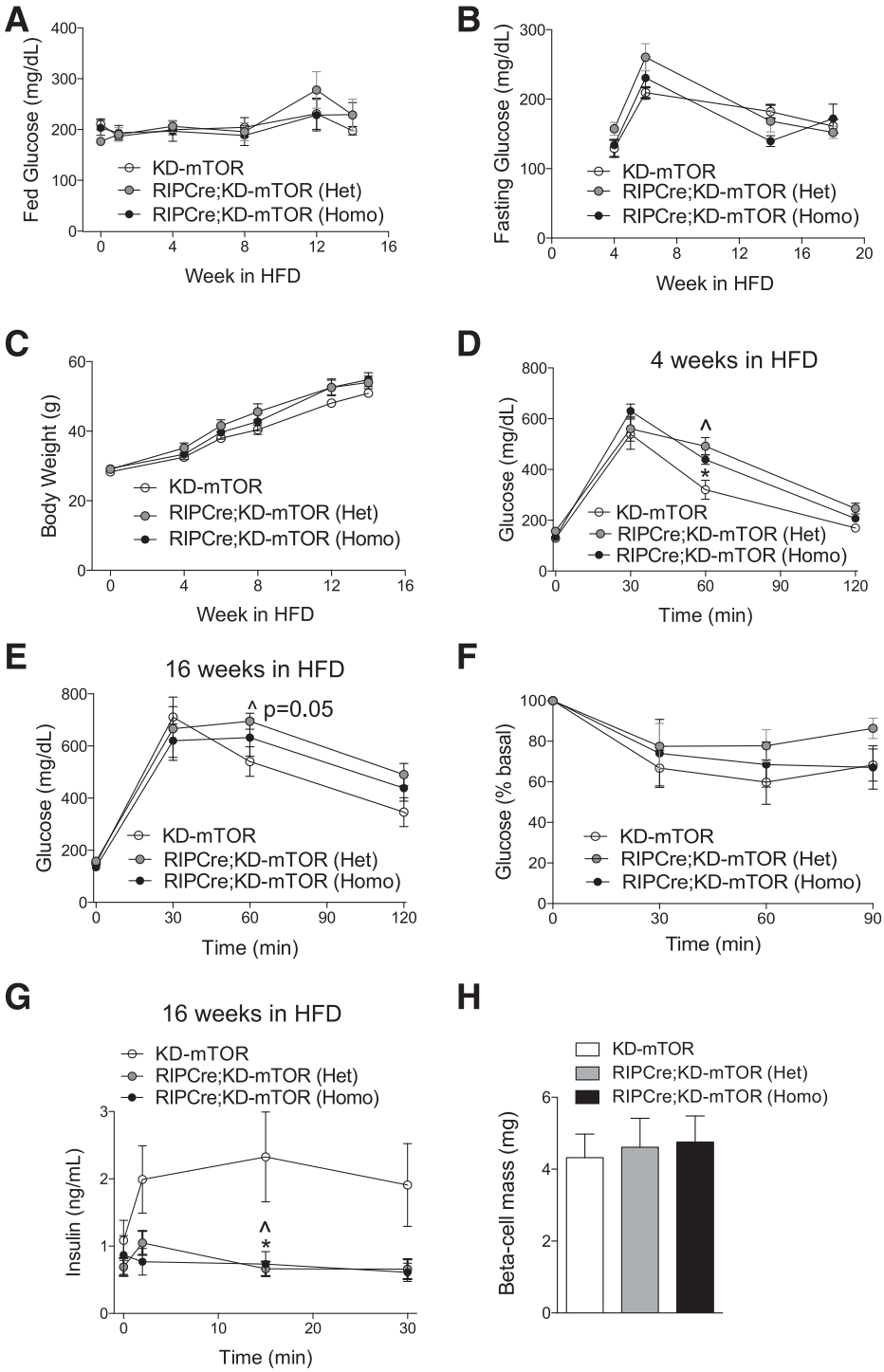

Figure 6—Abnormal adaptation of RIPCre;KD-mTOR mice to HFD. *A* and *B*: Random and fasting blood glucose during HFD. *C*: No differences in body weight were observed between genotypes. Both RIPCre;KD-mTOR (Het) and RIPCre;KD-mTOR (Homo) mice developed impaired glucose tolerance (*D* and *E*), insulin resistance (*F*), and blunted GSIS (*G*) in response to HFD in vivo. *H*: No alteration in β-cell mass in response to 16 weeks of HFD in vivo was observed between genotypes. Statistical analyses were conducted using two-way ANOVA for *D*, *E*, and *F*, and show significant genotype interaction in *D*. Individual time points were assessed by statistical analyses using unpaired, nonparametric Mann-Whitney *U* test. *$P < 0.05$ between RIPCre;KD-mTOR (Homo) and control mice; ^$P < 0.05$ between RIPCre;KD-mTOR (Het) and control mice; $n = 6$.

or HFD, suggesting that potential expression of the transgene in the hypothalamus was not sufficient to alter energy homeostasis in these mice. Unexpectedly, we did not observe any alteration in β-cell mass. Moreover, we found that RIPCre;KD-mTOR mice exhibited defective adaptation to HFD, mainly by alterations in insulin

secretion. Interestingly, we showed that defects in insulin secretion in RIPCre;KD-mTOR mice were caused in part by the decrease in Pdx-1 levels, identifying a novel mTOR–Pdx-1 axis in β-cells. Interestingly, the magnitude of the reduction in *Pdx-1*, *Ins1*, and *Ins2* mRNA levels was not sufficient to alter insulin content. This is not unexpected, as *Ins2*$^{-/-}$;*Ins1*$^{+/-}$ and *Pdx-1*$^{+/-}$ mice exhibit normal insulin content (21,23). These findings could be explained in part by the abundance and stability of *insulin* 2 mRNA, the large amount of stored insulin, and potential post-transcriptional or translational compensatory mechanisms. Finally, the lack of changes in insulin content in RIPCre;KD-mTOR mice was observed during normal conditions, and it is possible that insulin content defects could be uncovered after exposure of these mice to conditions of increased insulin demand, such as chronic hyperglycemia or insulin resistance.

The results of these experiments demonstrate that mTOR activity is essential for normal β-cell function. The normal calcium responses to glucose in RIPCre;KD-mTOR (Homo) mice suggested that the defects in insulin secretion occur distal to calcium influx and at the level of vesicle trafficking or function of exocytotic machinery proteins. It is possible that mTOR signaling could regulate expression of SNARE proteins at the transcriptional or translational level, and we plan to design experiments to test this hypothesis. In addition, the amplification pathway in islets expressing the KD-mTOR mutant appears intact, as demonstrated by conserved cAMP levels in response to glucose. The individual contribution of reductions in mTORC1 or mTORC2 signaling to the insulin secretory phenotype of RIPCre; KD-mTOR mice is unclear, but a role of mTORC2 is supported by previous evidence showing that mice with loss of mTORC2 signaling by inactivation of Rictor in β-cells exhibit alterations in insulin secretion (4). Downstream of mTORC2, activation of Akt signaling by S473 phosphorylation emerges as a potential mechanism. Support for a role of the mTORC2/Akt pathway in the regulation of insulin secretion comes from the observation that mice with reduction of Akt activity in β-cells exhibit an insulin secretory defect that is reminiscent of that observed in the RIPCre; KD-mTOR mice (24). How the mTORC2/Akt pathway regulates insulin secretion is not entirely clear, but it is possible that distal events that regulate vesicle trafficking and exocytosis are involved. In addition to Akt, the role of mTORC2 in actin filament remodeling (25–27) could also potentially alter vesicle trafficking or exocytosis. Moreover, it is also possible that the reduction in Pdx-1 contributes to the alterations in insulin secretion observed in RIPCre;KD-mTOR mice. Some of the defects in insulin secretion resemble the abnormalities described in Pdx-1 heterozygous mice (28), and it is likely that reduction of this critical transcription factor could alter β-cell function by regulating different biological functions. Finally, it is important to note that reductions in mTORC2, phosphorylated Akt, and Pdx-1 levels were associated with alteration in GSIS but not survival as demonstrated by TUNEL. Decrease in GSIS with conserved mass in these mice is reminiscent of the phenotype observed in mice with partial reduction of Akt activity in β-cells, suggesting that decrease in Akt activity in both models is not sufficient to alter β-cell survival (24). In addition, it is important to mention that three isoforms of Akt (Akt 1, 2, and 3) in β-cells contribute to total Akt activity, and the reduction of Akt1 activity demonstrated in these studies by S473 phosphorylation is not sufficient to reduce total Akt activity to a level that affects survival. In addition, it is possible that compensatory pathways can contribute to explain the lack of changes in β-cell mass and survival after decrease in mTOR activity.

In contrast to mTORC2, the evidence linking mTORC1 to the regulation of insulin secretion comes from studies using rapamycin. In general, rapamycin treatment reduces insulin secretion but the studies supporting this concept are less conclusive as the experiments use different concentrations and time of exposures. In addition, the inhibition of both mTORC1 and mTORC2 by prolonged incubation with this agent also limits some of the conclusions about the role of mTORC1 in insulin secretion. Finally, some studies suggest that rapamycin is a more efficient inhibitor of S6K and inefficiently and transiently inhibits eukaryotic translation initiation factor 4E binding protein (4E-BP) phosphorylation (29). Future studies using genetic models could uncover the effect of mTORC1 in insulin secretion.

The current study demonstrates a novel link between mTOR signaling and regulation of Pdx-1 levels. A potential explanation for a decrease in Pdx-1 levels in RIPCre;KD-mTOR mice is through inhibition of the mTORC2/Akt pathway. Further confirmation of this was supported by the reduction of Pdx-1 in islets from RIPCre;Rictor$^{fl/fl}$ but not islets in normoglycemic RIPCre;Raptor$^{fl/fl}$ mice. These data support the concept that loss of Pdx-1 protein is mediated by a mTORC2-dependent mechanism. However, the decrease in Pdx-1 levels observed in these studies was not sufficient to alter β-cell survival. Downstream of mTORC2, evidence in the literature suggests that Akt could be involved by regulating Pdx-1 degradation in a GSK3α-dependent manner (18,20,30). Other proteins such as Pdx-1 C terminus–interacting factor 1 (Pcif1) has also been demonstrated to modulate Pdx-1 protein stability (31); however, it is unknown how mTORC1 or mTORC2 could regulate Pcif1. In addition, our studies also showed that reduction of Pdx-1 levels in RIPCre;KD-mTOR mice appear to have a transcriptional component. How mTOR could regulate *Pdx-1* transcript is unclear. MafA and Foxa2 have been shown to regulate Pdx-1 transcription (32,33), but we found no differences in *MafA* mRNA in islets from RIPCre;KD-mTOR mice. Future studies using promoter reporter assays could further identify critical elements in the *Pdx-1* promoter and the transcription factors involved. It is also possible that mTORC1 plays a role, but we do not have any evidence for this mechanism.

The current study revealed that the islet architecture and β-cell mass, proliferation, and survival in RIPCre;KD-mTOR mice was conserved in neonates and in adults. In addition,

the β-cell mass adaptation of RIPCre;KD-mTOR mice to HFD was also conserved. These results are not surprising as the degree of mTOR signaling inhibition was partial, and it is likely that more severe β-cell mass phenotypes are observed in mice with complete loss of mTOR function in β-cells. It would be interesting to compare the RIPCre;KD-mTOR phenotype to that of conditional inactivation of mTOR in β-cells. In summary, these findings suggest that partial reduction in mTOR signaling is not essential for β-cell development and adaptation of β-cell mass to insulin resistance but is involved in regulating insulin secretion.

In summary, we have assessed the role of mTOR signaling in β-cells by developing an animal model with attenuation of both mTORC1 and mTORC2 signaling. Using this model, we uncovered that reduction in mTOR signaling plays an important role in insulin secretion but not β-cell mass. Thus, these studies extend our current knowledge on the mechanisms responsible for insulin secretion induced by nutrient and growth factor signals and identify mTOR as a critical component of this process in β-cells. Given the role of overnutrition on obesity-induced insulin resistance, this work also provides insight into how nutrient signals regulate β-cell adaptation to insulin resistance.

Acknowledgments. The authors thank Lauren See, Michelle Smith, Rebecca Barbaresso, Daniel Meister, and Seokwon Jo (Division of Metabolism, Endocrinology & Diabetes, Department of Internal Medicine, University of Michigan) for technical assistance.

Funding. This work was supported by National Institutes of Health grants R01 DK084236 and DK073716 (to E.B.-M.). A Career Development Award from the National Institute of Diabetes and Digestive and Kidney Diseases (K01-DK-103823) supported E.U.A. The National Institutes of Health Cellular and Molecular Biology Training Grant T32GM007315 supported N.B. This work was also supported by National Institutes of Health grant R01 DK46409 to L.S.

Duality of Interest. No potential conflicts of interest relevant to this article were reported.

Author Contributions. E.U.A. designed and performed experiments, analyzed data, interpreted results, and wrote and edited the manuscript. N.B., M.B.-R., M.A.W., and S.V. performed experiments and analyzed data. L.E. contributed to discussions. L.S. contributed to discussions on the calcium experiments. E.B.-M. conceived the project, developed the animal model, interpreted results, and reviewed, wrote, and edited the manuscript. E.B.-M. is the guarantor of this work and, as such, had full access to all the data in the study and takes responsibility for the integrity of the data and the accuracy of the data analysis.

References

1. Blandino-Rosano M, Chen AY, Scheys JO, et al. mTORC1 signaling and regulation of pancreatic β-cell mass. Cell Cycle 2012;11:1892–1902

2. Rachdi L, Balcazar N, Osorio-Duque F, et al. Disruption of Tsc2 in pancreaticbeta cells induces beta cell mass expansion and improved glucose tolerance in a TORC1-dependent manner. Proc Natl Acad Sci U S A 2008;105:9250–9255

3. Elghazi L, Balcazar N, Blandino-Rosano M, et al. Decreased IRS signaling impairs beta-cell cycle progression and survival in transgenic mice overexpressing S6K in beta-cells. Diabetes 2010;59:2390–2399

4. Gu Y, Lindner J, Kumar A, Yuan W, Magnuson MA. Rictor/mTORC2 is essential for maintaining a balance between beta-cell proliferation and cell size. Diabetes 2011;60:827–837

5. Sarbassov DD, Guertin DA, Ali SM, Sabatini DM. Phosphorylation and regulation of Akt/PKB by the Rictor-mTOR complex. Science 2005;307:1098–1101

6. Barlow AD, Nicholson ML, Herbert TP. Evidence for rapamycin toxicity in pancreatic β-cells and a review of the underlying molecular mechanisms. Diabetes 2013;62:2674–2682

7. Zahr E, Molano RD, Pileggi A, et al. Rapamycin impairs in vivo proliferation of islet beta-cells. Transplantation 2007;84:1576–1583

8. Lamming DW, Ye L, Katajisto P, et al. Rapamycin-induced insulin resistance is mediated by mTORC2 loss and uncoupled from longevity. Science 2012;335:1638–1643

9. Hamada S, Hara K, Hamada T, et al. Upregulation of the mammalian target of rapamycin complex 1 pathway by Ras homolog enriched in brain in pancreatic beta-cells leads to increased beta-cell mass and prevention of hyperglycemia. Diabetes 2009;58:1321–1332

10. Herrera PL. Adult insulin- and glucagon-producing cells differentiate from two independent cell lineages. Development 2000;127:2317–2322

11. Sekulić A, Hudson CC, Homme JL, et al. A direct linkage between the phosphoinositide 3-kinase-AKT signaling pathway and the mammalian target of rapamycin in mitogen-stimulated and transformed cells. Cancer Res 2000; 60:3504–3513

12. Miyazaki S, Miyazaki T, Tashiro F, Yamato E, Miyazaki J. Development of a single-cassette system for spatiotemporal gene regulation in mice. Biochem Biophys Res Commun 2005;338:1083–1088

13. Polak P, Cybulski N, Feige JN, Auwerx J, Rüegg MA, Hall MN. Adipose-specific knockout of raptor results in lean mice with enhanced mitochondrial respiration. Cell Metab 2008;8:399–410

14. Bentzinger CF, Romanino K, Cloëtta D, et al. Skeletal muscle-specific ablation of raptor, but not of rictor, causes metabolic changes and results in muscle dystrophy. Cell Metab 2008;8:411–424

15. Alejandro EU, Gregg B, Wallen T, et al. Maternal diet-induced microRNAs and mTOR underlie β cell dysfunction in offspring. J Clin Invest 2014;124:4395–4410

16. Offield MF, Jetton TL, Labosky PA, et al. PDX-1 is required for pancreatic outgrowth and differentiation of the rostral duodenum. Development 1996;122:983–995

17. Johnson JS, Kono T, Tong X, et al. Pancreatic and duodenal homeobox protein 1 (Pdx-1) maintains endoplasmic reticulum calcium levels through transcriptional regulation of sarco-endoplasmic reticulum calcium ATPase 2b (SERCA2b) in the islet β cell. J Biol Chem 2014;289:32798–32810

18. Boucher MJ, Selander L, Carlsson L, Edlund H. Phosphorylation marks IPF1/PDX1 protein for degradation by glycogen synthase kinase 3-dependent mechanisms. J Biol Chem 2006;281:6395–6403

19. Liu Z, Tanabe K, Bernal-Mizrachi E, Permutt MA. Mice with beta cell overexpression of glycogen synthase kinase-3beta have reduced beta cell mass and proliferation. Diabetologia 2008;51:623–631

20. Humphrey RK, Yu SM, Flores LE, Jhala US. Glucose regulates steady-state levels of PDX1 via the reciprocal actions of GSK3 and AKT kinases. J Biol Chem 2010;285:3406–3416

21. Johnson JD, Ahmed NT, Luciani DS, et al. Increased islet apoptosis in Pdx1+/- mice. J Clin Invest 2003;111:1147–1160

22. Cota D, Proulx K, Smith KA, et al. Hypothalamic mTOR signaling regulates food intake. Science 2006;312:927–930

23. Mehran AE, Templeman NM, Brigidi GS, et al. Hyperinsulinemia drives diet-induced obesity independently of brain insulin production. Cell Metab 2012;16: 723–737

24. Bernal-Mizrachi E, Fatrai S, Johnson JD, et al. Defective insulin secretion and increased susceptibility to experimental diabetes are induced by reduced Akt activity in pancreatic islet beta cells. J Clin Invest 2004;114:928–936

25. Qian Y, Corum L, Meng Q, et al. PI3K induced actin filament remodeling through Akt and p70S6K1: implication of essential role in cell migration. Am J Physiol Cell Physiol 2004;286:C153–C163

26. Cenni V, Sirri A, Riccio M, et al. Targeting of the Akt/PKB kinase to the actin skeleton. Cell Mol Life Sci 2003;60:2710–2720

27. Baker K, Kirkham S, Halova L, et al. TOR complex 2 localises to the cytokinetic actomyosin ring and controls the fidelity of cytokinesis. J Cell Sci 2016;129:2613–2624

28. Johnson JD, Bernal-Mizrachi E, Alejandro EU, et al. Insulin protects islets from apoptosis via Pdx1 and specific changes in the human islet proteome. Proc Natl Acad Sci U S A 2006;103:19575–19580

29. Choo AY, Blenis J. Not all substrates are treated equally: implications for mTOR, rapamycin-resistance and cancer therapy. Cell Cycle 2009;8:567–572

30. Semache M, Zarrouki B, Fontés G, et al. Per-Arnt-Sim kinase regulates pancreatic duodenal homeobox-1 protein stability via phosphorylation of glycogen synthase kinase 3β in pancreatic β-cells. J Biol Chem 2013;288:24825–24833

31. Claiborn KC, Sachdeva MM, Cannon CE, Groff DN, Singer JD, Stoffers DA. Pcif1 modulates Pdx1 protein stability and pancreatic β cell function and survival in mice. J Clin Invest 2010;120:3713–3721

32. Vanhoose AM, Samaras S, Artner I, Henderson E, Hang Y, Stein R. MafA and MafB regulate Pdx1 transcription through the Area II control region in pancreatic beta cells. J Biol Chem 2008;283:22612–22619

33. Lee CS, Sund NJ, Vatamaniuk MZ, Matschinsky FM, Stoffers DA, Kaestner KH. Foxa2 controls Pdx1 gene expression in pancreatic beta-cells in vivo. Diabetes 2002;51:2546–2551